Hindawi
Journal of Advanced Transportation
Volume 2021, Article ID 9945398, 13 pages
https://doi.org/10.1155/2021/9945398

Research Article

A Two-Level Model for Traffic Signal Timing and Trajectories Planning of Multiple CAVs in a Random Environment

Yangsheng Jiang,[1,2,3] Bin Zhao,[1,2] Meng Liu,[1,2] and Zhihong Yao[1,2,3,4]

[1]*School of Transportation and Logistics, Southwest Jiaotong University, Chengdu 610031, Sichuan, China*
[2]*National Engineering Laboratory of Integrated Transportation Big Data Application Technology, Southwest Jiaotong University, Chengdu 610031, Sichuan, China*
[3]*National United Engineering Laboratory of Integrated and Intelligent Transportation, Southwest Jiaotong University, Chengdu 610031, Sichuan, China*
[4]*Institute of System Science and Engineering, Southwest Jiaotong University, Chengdu 610031, Sichuan, China*

Correspondence should be addressed to Zhihong Yao; zhyao@my.swjtu.edu.cn

Received 10 March 2021; Revised 29 March 2021; Accepted 19 April 2021; Published 27 April 2021

Academic Editor: Linchao Li

Connected and automated vehicles (CAVs) trajectories not only provide more real-time information by vehicles to infrastructure but also can be controlled and optimized, to further save travel time and gasoline consumption. This paper proposes a two-level model for traffic signal timing and trajectories planning of multiple connected automated vehicles considering the random arrival of vehicles. The proposed method contains two levels, i.e., CAVs' arrival time and traffic signals optimization, and multiple CAVs trajectories planning. The former optimizes CAVs' arrival time and traffic signals in a random environment, to minimize the average vehicle's delay. The latter designs multiple CAVs trajectories considering average gasoline consumption. The dynamic programming (DP) and the General Pseudospectral Optimal Control Software (GPOPS) are applied to solve the two-level optimization problem. Numerical simulation is conducted to compare the proposed method with a fixed-time traffic signal. Results show that the proposed method reduces both average vehicle's delay and gasoline consumption under different traffic demand significantly. The average reduction of vehicle's delay and gasoline consumption are 26.91% and 10.38%, respectively, for a two-phase signalized intersection. In addition, sensitivity analysis indicates that the minimum green time and free-flow speed have a noticeable effect on the average vehicle's delay and gasoline consumption.

1. Introduction

Traffic congestion has become a common traffic phenomenon in many cities [1]. In the United States, the transportation sector consumed about 143 billion gallons of gasoline in 2017 [2]. Moreover, traffic congestion leads to additional transportation emissions and travel delays. In 2017, due to traffic congestion, drivers in the United States waste an average of 41 hours per year during peak hours [3]. Therefore, it is urgent to save gasoline consumption and travel time in cities [4, 5].

As one of the effective methods to alleviate urban traffic congestion [6], traffic signal control [7] first appeared in London, England, in 1868. Currently, traffic signal control mainly consists of three strategies: fixed-time control, vehicle-actuated control, and traffic signal adaptive control. These strategies allocate space-time right of way to vehicles in different conflict directions to resolve traffic flow conflicts at intersections [8]. However, these control strategies rely on traffic data from infrastructure-based vehicle detection systems, such as loop detectors, radar, or cameras [9–11]. Infrastructure-based vehicle detection systems only provide limited discrete data, and their installation and maintenance costs are considerably high [9]. Recently, with the development of wireless communication and automatic driving technologies, CAVs can realize the information exchange

between vehicles and infrastructure (i.e., traffic signal equipment) [12, 13]. Therefore, traffic signals and vehicle trajectories can be optimized and designed for connected automated vehicles (CAVs) to improve traffic efficiency and save gasoline consumption.

Many works have been conducted to search the optimal traffic signal and vehicle trajectories in the CAVs environment [14]. These works can be divided threefold. Firstly, a large number of signal control algorithms were proposed to optimize traffic signals with CAVs data [12, 15–20]. Secondly, many studies designed vehicle trajectories for CAVs to save gasoline consumption [21–26]. Thirdly, several methods focused on optimizing traffic signals and CAVs' trajectories to save travel time and gasoline consumption [8, 27–29].

However, there are several limitations to current integrated optimization methods. First, Feng et al. [8] and Yu et al. [29] only optimized the leading vehicle trajectory of a platoon and a car-following model that calculates the other vehicles' trajectories. Second, Xu et al. [28] proposed a vehicle trajectory designing model that considered a safe front vehicle distance. Still, they did not consider optimizing the trajectory of all CAVs at the same time. Therefore, this study would fill in this gap by showing a two-level model for traffic signal timing and trajectories planning of multiple connected automated vehicles considering the random arrival of vehicles.

The contribution of this paper consists of extending the optimal framework in Feng et al. [8]. First, instead of optimizing traffic signals by dynamic programming [8], we formulate an optimal arrival time calculation model for each CAV based on traffic signal timing and optimize traffic signals and vehicles' arrival time for random arrival CAVs to minimize average vehicle's delay. Second, unlike Feng et al. [8] and Yu et al. [29], only optimizing the leading vehicle trajectory of a platoon, the other vehicle trajectories are generated by a car-following model. Here, we proposed a multiple CAVs trajectories planning model, which is solved by the GPOPS [30]. Compared with Feng et al. [8], Yu et al. [29], and Xu et al. [28], the proposed model can optimize the trajectories of multiple CAVs at the same time. Third, we develop a two-level optimization framework and algorithm. Finally, we design the numerical examples and investigate the influence of critical parameters on the proposed method's performance.

The remainder of the paper is organized as follows. Section 2 reviews the research on traffic signal and trajectory optimization. Section 3 introduces some assumptions, two-level model, and solution algorithm. Section 4 presents numerical experiments, discussions, and sensitivity analysis. Finally, conclusions and recommendations are delivered in Section 5.

2. Literature Review

Connected and automated vehicles (CAVs) have great potential in improving traffic efficiency and reducing traffic congestion and have gained a wide application in the transportation field during the last decade [31]. These applications mainly focus on CAV-based trajectories planning [22, 23, 25, 26, 32–34] and CAV-based signal timing optimization [9, 12, 16, 35] and even further to design traffic signals and CAVs trajectories simultaneously [8, 27, 29, 34, 36, 37]. These studies showed that CAVs applications in trajectories planning and signal timing optimization could further reduce gasoline consumption, pollutant emissions, delays, and stops caused by more stable speed change and fewer stops at the intersection [38].

To our knowledge, the first approach focuses on vehicle trajectory planning [39, 40]. He et al. [32] proposed a speed optimization model to give ecodriving suggestions considering queues on a signalized arterial. Wan et al. [22] developed a speed advisory model (SAM) based on a given signal timing plan. Then, an analytical driving strategy is obtained to minimize fuel consumption. The results indicated that the SAM reduces fuel consumption and benefitted human-driven vehicles (HDVs), and the platoon fuel consumption decreased with the increase of CAVs' penetration rates. Zhao et al. [25] designed an ecological driving strategy to coordinate the platoon mixed with CAVs and HDVs. A model predictive control is proposed to save platoons' fuel consumption with a fixed-time traffic signal. The results showed that the driving strategy could further smooth out the trajectory and save fuel consumption. Therefore, these studies mainly focus on optimizing CAVs trajectories based on a preset traffic signals.

The second method optimizes signal timing plans by CAVs data [41, 42]. Goodall et al. [35] optimized traffic signal with a predictive microscopic simulation algorithm (PMSA). The connected vehicles (CVs) data, including locations and speeds, were used to predict future traffic conditions via the microscopic simulation method. A 15-second rolling horizon was chosen to minimize vehicles' delay, stops, and decelerations. Feng et al. [9] presented a real-time traffic adaptive signal control algorithm to minimize vehicle delay and queue length via connected vehicle (CVs) data. The simulation results indicated that the proposed algorithm reduced vehicle delay and balanced each phase's queue length. However, they did not consider optimizing the CAVs trajectories at the same time.

Therefore, to address this gap, the third approach simultaneously optimizes CAVs trajectories and traffic signals. Xu et al. [28] presented a two-level method to optimize traffic signal and speed for CAVs. The first level optimized traffic signals and CAVs arrival times to minimize travel time; the second level planned CAVs trajectories to save individual vehicles' fuel consumption. The results indicated that this method could improve transportation efficiency and fuel economy significantly. Yu et al. [29] developed mixed-integer linear programming to optimize vehicle trajectories and traffic signals at a signalized intersections. Simulation results showed that this method was superior to actuated control in vehicle's delay, intersection capacity, and CO_2 emission. Feng et al. [8] proposed a two-stage method with traffic signal optimization and vehicle trajectory planning. The optimal control theory and dynamic programming (DP) are applied to optimize vehicle trajectories and traffic signals to minimize vehicle delay and fuel

consumption. Results showed that the proposed method could reduce vehicle delay and fuel consumption under different demand compared to fixed-time traffic signal control. However, these joint optimization methods only optimize the trajectory of the leading vehicle in a platoon; a car-following model is used to calculate the other vehicle's trajectory in the platoon. Ghiasi et al. [27] considered the joint optimization algorithm's computational efficiency; an analytical solution to joint CAVs trajectories and traffic signals optimization problem was proposed in their study. The numerical experiment showed that the proposed model could reduce travel delay and fuel consumption significantly.

This study proposes a two-level model for traffic signal timing and trajectories planning of multiple CAVs considering the random arrival of vehicles. The integrated optimization problem is modeled as a two-level model. Firstly, the traffic signal and arrival time for CAVs are optimized by the signal timing model to minimize the average vehicle's delay. Secondly, considering average gasoline consumption, an optimal control method is proposed to optimize trajectories for all CAVs. Finally, the proposed method is tested in a simulation experiment, and numerical studies and sensitivity analysis are carried out based on a simple two-phase intersection.

3. Methodology

3.1. Assumption. The following necessary assumptions are made to facilitate modeling and analysis.

(1) The interarrival time of all CAVs follows the shifted negative exponential distribution, which is verified at an isolated intersection [8, 21, 29]. This means CAVs arrive at the border of the control zone following a Poisson distribution.

(2) All CAVs can share information (such as location, speed, and arrival time) through V2V; hence, their arrival time can be predicted more accurately [25].

(3) All CAVs arrive at the boundary of the control zone and through the downstream intersection with the desired speed, which can refer to Ghiasi et al. [27].

(4) All CAVs cannot change lanes in the control zone; that is, only the longitudinal movement is considered [43–45].

3.2. Problem Statement. In this study, no left-turn and right-turn are considered; only through traffic flow it is modeled, which is shown in Figure 1. There are four arms indexed by $i \in \mathcal{I} = \{1, 2, 3, 4\}$, and l_i and v_i^f are the length of the control zone and the desired speed of arm i, $i \in \mathcal{I}$, respectively. A simple two-phase signal timing plan and an arm i as an example are shown in Figure 2; the traffic signal is $\mathcal{S} = \{G_1, G_2, G_3, G_4\}$ or $\mathcal{S} = \{R_1, R_2, R_3, R_4\}$, where G_i and R_i are the effective green time and red time for arm i, $i \in \mathcal{I}$, respectively. In this study, the indexes 1, 2, 3, and 4 are defined as east, south, west, and north arm, respectively. Therefore, there have $G_1 = G_3$ and $G_2 = G_4$. Let $L = R_1 + R_2 - G_1 - G_2$ represent the lost time of a traffic signal cycle. The traffic

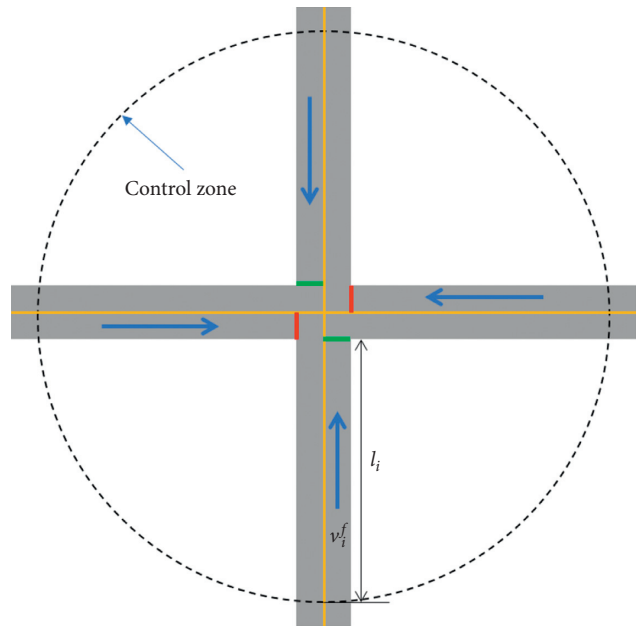

Figure 1: A simple intersection with four arms.

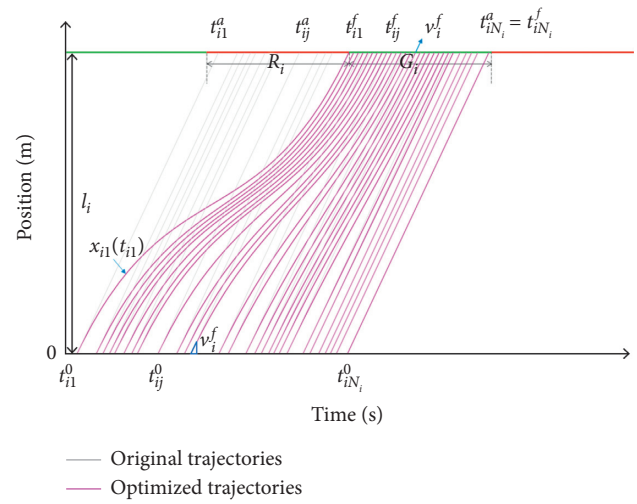

Figure 2: The vehicle trajectories planning of each arm $i.i \in \mathcal{I}$.

arrival rate and the saturation flow rate of arm i are defined as λ_i and μ_i. The unsaturated traffic is considered in this study, which can be expressed as $\sum_{i \in \mathcal{I}} (\lambda_i (R_i + G_i)/\mu_i G_i) < 1$. For the convenience of the readers, the main variables used in this paper are shown in Table 1.

As shown in Figure 2, CAVs arrival at the border of the control zone is defined as $j \in \mathcal{N}_i = \{1, 2, \ldots, N_i\}$, $i \in \mathcal{I}$. Let $\mathcal{X}_i = \{x_{ij}(t_{ij})\}$ be the set of CAV trajectories at each arm i, where $x_{ij}(t_{ij})$ is the position of the j-th CAV at each arm i at time t_{ij}. $\dot{x}_{ij}(t_{ij})$ and $\ddot{x}_{ij}(t_{ij})$ are the instantaneous speed and acceleration of the j-th CAV at each arm i at time t_{ij}, respectively. Let t_{ij}^a and t_{ij}^f be the expected and optimal arrival times of the j-th CAV at the stop line of each arm i. t_{ij}^0 is the time of j-th CAV arriving at the border of the control zone at each arm i, which can be estimated accurately via advanced CAV technology [27].

Table 1: Notation of major symbols used in this paper.

Symbol	Description
Gasoline consumption	
α	The parameter of gasoline consumption rate
M	The weight of the vehicle
β_1	The parameter relevant to the energy efficiency of the engine
β_2	The parameter associated with positive acceleration
v	The vehicle's speed
a	The vehicle's acceleration
$P(t)$	The power (kW) required to drive the vehicle
Traffic signals	
$\mathcal{F}$	Set of arms at the intersection
$\mathcal{S}$	A signal timing plan
G_i	The effective green time for arm i
R_i	The effective red time for arm i
L	The lost time of a traffic signal cycle
l_i	The length of the control zone at arm i
v_i^f	The desired speed at each arm i, which is equal to free-flow speed
λ_i	The vehicle arrival rate at arm i
μ_i	The saturation flow rate at arm i
$G_i^{\min}$	The minimum green time duration for arm i
$G_i^{\max}$	The maximum green time duration for arm i
Vehicle trajectory	
$\mathcal{N}_i$	The set of CAVs arriving at the border of control zone at arm i
$\mathcal{X}_i$	The set of CAVs trajectories functions at arm i
$x_{ij}(t_{ij})$	The location of the j-th CAV at arm i at time t_{ij}
$\dot{x}_{ij}(t_{ij})$	The speed of the j-th CAV at arm i at time t_{ij}
$\ddot{x}_{ij}(t_{ij})$	The acceleration of the j-th CAV at arm i at time t_{ij}
t_{ij}^0	The time of j-th CAV arriving at the border of control zone at arm i
t_{ij}^a	The expected arrival time at the stop line of the j-th CAV at arm i
t_{ij}^*	The optimal arrival time at the stop line of the j-th CAV at arm i
τ	The delay of control and communication
s_0	The safety spacing between two consecutive CAVs
$a_{\min}$	The minimum acceleration of CAVs
$a_{\max}$	The maximum acceleration of CAVs

3.3. Model Formulation. The proposed method consists of two levels, i.e., vehicle's arrival time and traffic signal timing, and vehicle trajectories planning. The former optimizes traffic signals and vehicles' arrival time for CAVs to minimize the average vehicle's delay. The latter optimizes trajectories for all CAVs considering average gasoline consumption based on the optimal traffic signal timing plan. To better understand the proposed model, the vehicle's trajectories are optimized by giving the optimal traffic signal plan of a two-phase intersection: $\mathcal{S} = \{G_1, G_2, G_3, G_4\}$ or $\mathcal{S} = \{R_1, R_2, R_3, R_4\}$. Here, $G_1 = G_3$, $G_2 = G_4$ and $L = R_1 + R_2 - G_1 - G_2$.

3.3.1. Optimal Arrival Time. The time of CAVs (t_{ij}^0) arriving at the control zone border can be accurately estimated via the CAV technology [27]. Then, the expected arrival time of the j-th CAV arrival at the stop line of arm i can be estimated by

$$t_{ij}^a = t_{ij}^0 + \frac{l_i}{v_i^f}, \quad \forall i \in \mathcal{F}, j \in \mathcal{N}_i, \tag{1}$$

where the red signal is defined as the cycle starts is shown in Figure 2. Therefore, the number of CAVs arrival at this cycle ($N_i = |\mathcal{N}_i|$) is determined by the number of t_{ij}^a, which is determined by the arrival flow rate (λ_i).

The analysis indicates that the optimal arrival time at the stop line is determined by the expected arrival times, traffic signals, and saturation flow rate. Taking the optimal arrival time of the j-th CAV at each arm i as an example, it can be divided into the following four cases.

(a) The first CAV of a signal cycle at each arm i:

(i) If the expected arrival time of the first CAV is during the red signal period, to minimize the vehicle's delay, the first CAV's optimal arrival time is equal to the start time of the green signal in the next signal cycle.

(ii) If the expected arrival time of the first CAV is during the green signal duration, to minimize the vehicle's delay, the first CAV's optimal arrival time is equal to the expected arrival time.

(b) The other CAVs of a signal cycle at each arm i: the estimated arrival time is the sum of the optimal arrival time of the preceding CAV and saturation headway.

(i) If the estimated arrival time is shorter than the expected arrival time, the optimal arrival time is equal to the expected arrival time at the stop line.
(ii) If the estimated arrival time is not shorter than the expected arrival time, the optimal arrival time is equal to the estimated arrival time.

$$t_{ij}^{f} = \begin{cases} t_{i(j-1)}^{f} + \dfrac{1}{\mu_i}, & \text{if } t_{ij}^{a} \le t_{i(j-1)}^{f} + \dfrac{1}{\mu_i} \\ t_{ij}^{a}, & \text{if } t_{ij}^{a} > t_{i(j-1)}^{f} + \dfrac{1}{\mu_i} \end{cases}, \quad \forall i \in \mathcal{I}, j \in \mathcal{N}_i \setminus \{1\}. \tag{3}$$

3.3.2. Objective Function. (1) Vehicle's Delay Function. The travel delay of each CAV is defined as the difference between the actual and the free travel time. The free and actual travel time can be determined by (1) and (3), respectively. As a result, the vehicle's delay function for arm i is formulated as

$$\mathcal{D}_i(\mathcal{S}, \mathcal{X}_i) = \frac{1}{N_i} \sum_{j \in \mathcal{N}_i} \left(t_{ij}^{f} - t_{ij}^{a} - \frac{l_i}{v_i^{f}} \right), \quad \forall i \in \mathcal{I}, \tag{4}$$

where $\mathcal{D}_i$ is the average vehicle's delay for each arm i.

Therefore, the average vehicle's delay for this intersection is formulated as

$$\mathcal{D}(\mathcal{S}, \mathcal{X}) = \frac{1}{\sum_{i \in \mathcal{I}} N_i} \sum_{i \in \mathcal{I}} \sum_{j \in \mathcal{N}_i} \left(t_{ij}^{f} - t_{ij}^{a} - \frac{l_i}{v_i^{f}} \right). \tag{5}$$

(2) Gasoline Consumption Function. Gasoline consumption is a function of instantaneous speed and acceleration of vehicle [46–48], which is formulated as

$$F(v, a; t) = \begin{cases} \alpha + \beta_1 R_T(t) v(t) + \max\left\{0, \dfrac{\beta_2 M a^2(t) v(t)}{1000}\right\}, & \text{if } R_T(t) > 0, \\ \alpha, & \text{if } R_T(t) \le 0, \end{cases} \tag{6}$$

where α represents constant idle fuel rate (ml/s), M represents the weight of the vehicle (kg), β_1 and β_2 represent the efficiency parameters, a and v represent instantaneous acceleration and speed of a vehicle, respectively, and $R_T(t)$ represents total "tractive" force required to drive the vehicle, which is defined as

$$R_T(t) = b_1 + b_2 v(t) + b_3 v^2(t) + \frac{Ma(t)}{1000} + 9.81 \times 10^{-5} MG. \tag{7}$$

where b_1, b_2, and b_3 represent rolling, engine, and aerodynamic drag, respectively; G is percent grade. Referring to Akcelik [47], the calibrated parameters in (6) and (7) are M = 1600 kg, $G = 0$, $\alpha = 0.666$ ml/kJ, $\beta_1 = 0.0717$ ml/kJ, $\beta_2 = 0.0344$ ml/(kJ · m/s^2), $b_1 = 0.269$ kN, $b_2 = 0.0171$ kN (m/ s^2), $b_3 = 0.000672$.

The average gasoline consumption function for arm i is defined as

$$\mathcal{G}_i(\mathcal{S}, \mathcal{X}_i) = \frac{1}{N_i} \sum_{j \in \mathcal{N}_i} \int_{t_{ij}^{0}}^{t_{ij}^{f}} F\left(\dot{x}_{ij}(t), \ddot{x}_{ij}(t); t\right) \mathrm{d}t, \quad \forall i \in \mathcal{I}, \tag{8}$$

where $\mathcal{G}_i$ is the average gasoline consumption for arm i.

Therefore, the average gasoline consumption for this intersection is formulated as

$$\mathcal{G}(\mathcal{S}, \mathcal{X}) = \frac{1}{\sum_{i \in \mathcal{I}} N_i} \sum_{i \in \mathcal{I}} \sum_{j \in \mathcal{N}_i} \int_{t_{ij}^{0}}^{t_{ij}^{f}} F\left(\dot{x}_{ij}(t), \ddot{x}_{ij}(t); t\right) \mathrm{d}t. \tag{9}$$

3.3.3. Constrain Conditions

(1) Traffic Signals Constrain. The green time duration constraints: the green time duration of each arm i must be between the minimum and maximum green time duration.

$$G_i^{\min} \le G_i \le G_i^{\max}, \quad \forall i \in \mathcal{I}, \tag{10}$$

where $G_i^{\min}$ and $G_i^{\max}$ are the minimum and maximum green time duration for arm i, respectively.

The Signal Cycle Constraint. The sum-up of effective red time duration for all phases must equal the sum up of effective green time duration and constant lost time.

$$R_1 + R_2 = G_1 + G_2 + L. \tag{11}$$

The Unsaturated Traffic Flow Constraint. The maximum number of the departure CAVs must not be smaller than the number of the arrival CAVs for each arm i.

$$\lambda_i(R_i + G_i) \le \mu_i G_i, \quad \forall i \in \mathcal{I}. \tag{12}$$

(2) Vehicle Trajectories Constrain. Dynamic state constraint: at arm i, the position, velocity, and acceleration of the j-th CAV at any time should satisfy the following dynamic equations.

$$\dot{x}_{ij}(t) = \frac{\mathrm{d}x_{ij}(t)}{\mathrm{d}t}, \quad \forall t \in \left[t_{ij}^{0}, t_{ij}^{f}\right], i \in \mathcal{I}, j \in \mathcal{N}_i,$$

$$\ddot{x}_{ij}(t) = \frac{\mathrm{d}\dot{x}_{ij}(t)}{\mathrm{d}t}, \quad \forall t \in \left[t_{ij}^{0}, t_{ij}^{f}\right], i \in \mathcal{I}, j \in \mathcal{N}_i. \tag{13}$$

Initial Boundary Constraint. At arm i, the position, velocity, and acceleration of the j-th CAV at start time are given by the assumptions [27].

$$x_{ij}\left(t_{ij}^{0}\right) = 0, \quad \forall i \in \mathcal{I}, j \in \mathcal{N}_i,$$
$$\dot{x}_{ij}\left(t_{ij}^{0}\right) = v_i^f, \quad \forall i \in \mathcal{I}, j \in \mathcal{N}_i, \left(t_{ij}^{0}\right) = 0, \quad \forall i \in \mathcal{I}, j \in \mathcal{N}_i.$$
$$\ddot{x}_{ij} \tag{14}$$

Final Boundary Constraint. At arm i, the position, velocity, and acceleration of the j-th CAV at end time are given by the assumptions [27].

$$x_{ij}\left(t_{ij}^{f}\right) = l_i, \quad \forall i \in \mathcal{I}, j \in \mathcal{N}_i,$$
$$\dot{x}_{ij}\left(t_{ij}^{f}\right) = v_i^f, \quad \forall i \in \mathcal{I}, j \in \mathcal{N}_i, \left(t_{ij}^{f}\right) = 0, \quad \forall i \in \mathcal{I}, j \in \mathcal{N}_i.$$
$$\ddot{x}_{ij} \tag{15}$$

Consecutive Vehicle Position Constraint. The adjacent CAVs must meet the specific safety headway because of control and communication delay. The headway between vehicle $(j-1)$'s location with a control and communication delay τ ago $x_{i(j-1)}(t-\tau)$ and vehicle j's location, $x_{ij}(t)$ is no less than s_0 in time interval $[t_{i(j-1)}^{0}, t_{ij}^{f}]$.

$$x_{i(j-1)}(t-\tau) - x_{ij}(t) \geq L + s_0, \quad \forall i \in \mathcal{I}, n \in \mathcal{N}_i \setminus \{1\}, t_{ij} \in \left[t_{i(j-1)}^{0}, t_{ij}^{f}\right], \tag{16}$$

where τ is control and communication delay, s_0 is the safety spacing between two adjacent CAVs, and$L$ is the length of CAVs.

Speed Constraint. The speed of all CAVs cannot go beyond the free speed limit.

$$0 \leq \dot{x}_{ij}(t) \leq v_i^f, \quad \forall t \in \left[t_{ij}^{0}, t_{ij}^{f}\right], i \in \mathcal{I}, j \in \mathcal{N}_i. \tag{17}$$

Acceleration Constraint. The acceleration of all CAVs must be between the minimum and maximum acceleration.

$$a_{\min} \leq \ddot{x}_{ij}(t) \leq a_{\max}, \quad \forall t \in \left[t_{ij}^{0}, t_{ij}^{f}\right], i \in \mathcal{I}, j \in \mathcal{N}_i, \tag{18}$$

where $a_{\min}$ and $a_{\max}$ are the minimum and maximum acceleration, respectively.

3.4. Solution Method. In this study, a dynamic programming (DP) algorithm and the GPOPS are adopted to solve the traffic signal timing problem and multiple vehicle trajectories planning problem, respectively.

3.4.1. Dynamic Programming. Many DP-based traffic signal timing methods have been developed [8, 9, 49]. In the DP algorithm, state variables and decision variables are the key parameters. Equations (19)–(20) illustrate the relationship between the two parameters; see more details in [49].

$$s_p = s_{p-1} + h\left(x_p\right), \tag{19}$$

$$h\left(x_p\right) = \begin{cases} 0, & \text{if } x_p = 0, \\ x_p + r_p, & \text{otherwise}, \end{cases} \tag{20}$$

where s_p is the total number of time intervals from the beginning stage to the end of stage p and x_p and r_p are the green and the clearance time intervals of the stage p.

When the state variable s_p is given, the feasible set of decision variables can be calculated by

$$X_p\left(s_p\right) = \begin{cases} 0, & if\ s_p - r_p < x_{\min}, \\ \{x_{\min}, x_{\min}+1, \ldots, x_{\max}\}, & if\ s_p - r_p \geq x_{\min} \text{ and } T - s_{p-1} - r_p > x_{\max}, \\ \{x_{\min}, x_{\min}+1, \ldots, T - s_{p-1} - r_p\} & if\ T - s_{p-1} - r_p \leq x_{\max}. \end{cases} \tag{21}$$

After determining $X_p(s_p)$, DP is adopted to search for the optimal decision variables x_p. The DP algorithm consists of two recursions; the first recursion obtains the optimal objective function in every time interval; the second recursion searches the decision variables corresponding to the optimal objective.

3.5. Forward Recursion

(i) Step 1: Set initial stage $p = 1$, state variable $s_{p-1} = 0$, and value function $v_p(s_{p-1}) = 0$.

(ii) Step 2: For $s_p = 1, 2, \ldots, T$\{

$v_p(s_p) = \min\{f_p(s_p, x_p) + v_{p-1}(s_{p-1}) | x_p \in \mathbf{X}_p(s_p)\}$

$x_p^*(s_p) = \operatorname{argmin}_{x_p}\{f_p(s_p, x_p) + v_{p-1}(s_{p-1}) | x_p \in \mathbf{X}_p(s_p)\}$

Record $x_p^*(s_p)$ and $v_p(s_p)$ as the optimal solution and value function\}.

(iii) Step 3: If $(p < |P|)$, let$p = p + 1$, and go to Step 2.

Else if $(v_{p-k}(T) = v_p(T))$ for all $k \leq |P| - 1$, STOP.

Else $p = p + 1$, go to Step 2.

The first recursion starts with stage 1 and the cumulative value function as 0. For each stage, the DP searches the optimal solution $x_p^*(s_p)$ with a given state variable s_p. The

objective function $f_p(s_p, x_p)$ is determined by the expected arrival time (1) of all CAVs. The stop criteria for the first recursion are derived from Sen and Head [49]. Besides, the number of phases $|P|$ is 2 in this study, which contains the east-west phase and the north-south phase.

3.6. Backward Recursion. After optimal value function is determined, the optimal decision $x_p^*(s_p)$ of each stage can be retrieved in the second recursion as follows.

(i) **Step 1:** Set the optimal stages as J, and the optimal state variable $s_{J-1}^* = T$.

(ii) **Step 2:** For $p = J-1, J-2, \ldots, 1\{$

Finding $x_p^*(s_p^*)$ from the records of **Forward recursion.**

If $(j > 1)$, $s_{p-1}^* = s_p^* - h_p(x_p^*(s_p^*))\}$.

3.6.1. General Pseudospectral Optimal Control Method. As an optimal control problem, the vehicle trajectories planning can be handled numerically by GPOPS [30], which is widely used in vehicle trajectory optimization [25, 32, 33]. Therefore, the GPOPS is used to solve the optimal control problem for multiple CAVs trajectory planning.

3.6.2. Solution Algorithm. In summary, the two-level optimization algorithm is as follows. (i.e., Algorithm 1).

4. Numerical Studies

4.1. Simulation Settings. The simulation duration of every scenario with a different traffic volume is 900 seconds. Every scenario is repeated five times with different random seeds. Besides, vehicle arrival conforms to the Poisson distribution [8, 21, 29].

In signal optimization, a four-arm and two phases of a cycle are selected. The time planning horizon is $T_p = 50$ s. The minimum and maximum green time are $G_i^{\min} = 15$ s and $G_i^{\max} = 30$ s, respectively. The lost time of each phase $(L/2) = 1$ s. The length of the control zone at each arm $l_i = 300$ m, and the free flow and the desired speed at each arm $v_i^f = 15$ m/s. The saturation flow rate of each arm $\mu_i = 1$ veh/s, which must be less than $1/(s_0/v_i^f) = 3$ veh/s in this study.

In the vehicle trajectories planning, the delay of control and communication $\tau = 0.1$ s. The safety spacing between two consecutive CAVs $s_0 = 5$ m. The length of CAVs $L = 5$ m. The minimum and maximum acceleration are $a_{\min} = -6\,\text{m/s}^2$ and $a_{\max} = 3\,\text{m/s}^2$, respectively.

4.2. Results and Discussions. The two-level integrated optimization model, denoted as "IO", is compared with Signal-fixed. Three volume levels, namely, 600, 800, and 1200 vph, are created in this study [50]. The demands in the two approaches (i.e., arm 1 and 3, arm 2 and 4) are set to be the same. To consider the difference in traffic between the two directions, we designed four scenarios, including two balanced and two unbalanced flows. In the "IO" control, vehicle trajectories are optimized by GPOPS [30], and the DP algorithm optimizes the signal timing plan in different scenarios. In the "Signal-fixed" control, vehicle trajectories are optimized by GPOPS [30], and the signal timing plan is optimized by Synchro [51] in different scenarios. Specifically, the signal parameters setup is the same as "IO" (e.g., the lost time of each phase, the saturation flow rate, and the minimum and maximum green time). The average vehicle's delay and gasoline consumption of 4 scenarios with different traffic demands are shown in Table 2. Besides, all CAVs trajectories and traffic signal plans can be obtained. Figure 3 shows vehicle trajectories for 4 scenarios with different demand.

As shown in Table 2, there are four scenarios, namely, 1200/1200, 1200/800, 800/800, and 800/600 vph. The simulation results show a significant decrease in the average vehicle's delay and gasoline consumption when IO control is applied. Compared with the Signal-fixed, the reduced average vehicle's delay with four scenarios are 26.91%, 15.57%, 24.17%, and 21.77%, and the reduced gasoline consumption with four scenarios are 10.38%, 5.30%, 8.50%, and 7.15%. In other words, the proposed integrated optimization method can averagely improve the transportation efficiency by 21.77% and decrease gasoline consumption by 7.83%, compared with Signal-fixed control in these studied scenarios, respectively.

Figure 3 shows that all CAVs pass through the intersection at free speed without stopping. Therefore, no CAVs are queuing at the stop line of the intersection. Furthermore, this method eliminates the loss of green start-up time compared with no trajectory optimization, and more vehicles can pass through the intersection in the same green interval. Besides, compared with Signal-fixed control, IO control has a smaller vehicle delay and gasoline consumption. This indicates that the integrated optimization method can better consider traffic signal and vehicle trajectories optimization, thus further reducing the average vehicle's delay and gasoline consumption, compared with Signal-fixed control. In addition, the minimum green time duration is considered in this study. Therefore, a part of the green time duration of the phase is wasted in Figure 3.

4.3. Sensitivity Analysis. In this study, the minimum green time $(G_i^{\min})$ and free-flow speed (v_i^f) are the most critical parameters. Therefore, we have carried on the analysis and the discussion of these two parameters.

4.3.1. Minimum Green Time. Minimum green time is to ensure the safety of drivers and pedestrians. A minimum green time that is too long may result in increased delay; one that is too short may violate pedestrian needs. Therefore, different geometric shapes of intersections can set different minimum green time. To avoid the influence of other parameters, scenario one (1200/1200 vph) is selected as a sensitivity analysis of the minimum green time. In the sensitivity analysis, $G_i^{\min}$ varies from 10 s to 20 s with an

Initialize:
(1)Set the total simulation time as T, the time planning horizon as T_p, the current time as $T_c = 0$, L, λ_i, μ_i, $G_i^{\min}$, $G_i^{\max}$, l_i, v_i^f in arm i,$\forall i \in \mathcal{I}$.
(2)Simulate the arrival times of CAVs at arm i,$\forall i \in \mathcal{I}$.
Iterate:
(3) **While** $T_c + T_p \leq T$ **do**
(4) Get the arrival times (t_{ij}^0, $\forall i \in \mathcal{I}$, $j \in \mathcal{N}_i$) of CAVs in time planning horizon $[T_c, T_c + T_p]$.
(5) Calculate t_{ij}^a, $\forall i \in \mathcal{I}$, $j \in \mathcal{N}_i$ based on equation (1).
(6) Optimize the traffic signal timing plan by DP algorithm.
(7) **For Each** signal cycle **do**
(8) Obtain signal time plan $\mathcal{S}$.
(9) **For** $i = 1 \longrightarrow 4$ **do**
(10) Obtain $\mathcal{N}_i$, t_{ij}^0, t_{ij}^a, $\forall i \in \mathcal{I}$, $j \in \mathcal{N}_i$.
(11) Calculate t_{ij}^f, $\forall i \in \mathcal{I}$, $j \in \mathcal{N}_i$.
(12) Optimize the j-th CAV trajectory by GPOPS.
(13) Save the vehicle trajectories $\mathcal{X}_i$ for the i arm.
(14) Calculate $\mathcal{G}_i$ and $\mathcal{D}_i$.
(15) **End**
(16) Calculate $\mathcal{D}$ and $\mathcal{G}$.
(17) **End**
(18) Save vehicle trajectories, signal timing plan, gasoline consumption, and average delay at the current time planning horizon $[T_c, T_c + T_p]$.
(19) $T_c = T_c + T_p$
(20) **End**
Output:
(21) Output vehicle trajectories, signal timing plan, gasoline consumption, and average delay at the total time planning horizon $[0, T]$.

Algorithm 1

increment of 1 s. The sensitivity analysis result is shown in Figure 4.

As shown in Figure 4, the sensitivity analysis result shows that a shorter minimum green time results in a significantly less average vehicle's delay and gasoline consumption under IO control. In the unsaturated traffic flow, a shorter minimum green time can ensure that CAVs pass through intersections faster, resulting in less travel time, deceleration, and acceleration. This is because a shorter minimum green time helps avoid the waste of green time caused by the random arrival of vehicles, especially in low traffic flow rates. As a result, there are a smaller average vehicle's delay and lower gasoline consumption.

4.3.2. Free-Flow Speed. The free-flow speeds influence CAVs arrival time, which is an essential parameter for traffic signal optimization and trajectories planning of this study. Scenario no.1 (1200/1200 vph) is selected as a sensitivity analysis of the free-flow speeds. In the sensitivity analysis, v_i^f is from 10 m/s to 20 m/s in steps of 1 m/s. The sensitivity analysis result is shown in Figure 5.

The sensitivity analysis (Figure 5) shows that the average vehicle's delay decreases with free-flow speed. This indicates that a more significant free speed resulting in shorter travel times of CAVs would lead to smaller vehicle delays. However, Figure 5 indicates the average gasoline consumption decreases with free-flow speed (10–13 m/s) before reaching the lowest point when the free speed is 13 m/s and then starts to increase. This suggests an optimal free-flow speed to minimize the average gasoline consumption, and the optimal free-flow speed is 13 m/s in this scenario.

5. Conclusions and Future Work

This study developed a two-level model for traffic signal timing and trajectories planning of multiple connected automated vehicles considering the random arrival of vehicles. Based on the numerical experiments, the following conclusions can be drawn:

(1) Compared with the Signal-fixed, the reduced average vehicle's delays with four scenarios are 26.91%, 15.57%, 24.17%, and 21.77%, and the reduced gasoline consumption with four scenarios are 10.38%, 5.30%, 8.50%, and 7.15%.

(2) The proposed two-level model could reduce both vehicle's delay and gasoline consumption by 26.91% and 10.38%, compared with Signal-fixed control in these studied scenarios, respectively.

(3) Sensitivity analysis suggests that the minimum green time and free speed have a significant impact on the two-level model's performance.

(4) A shorter minimum green time results in a significantly less average vehicle's delay and gasoline consumption. The optimal free-flow speed is 13 m/s in the study scenario.

In the current work, this work applied the proposed model to a single intersection, similar to vehicle merging

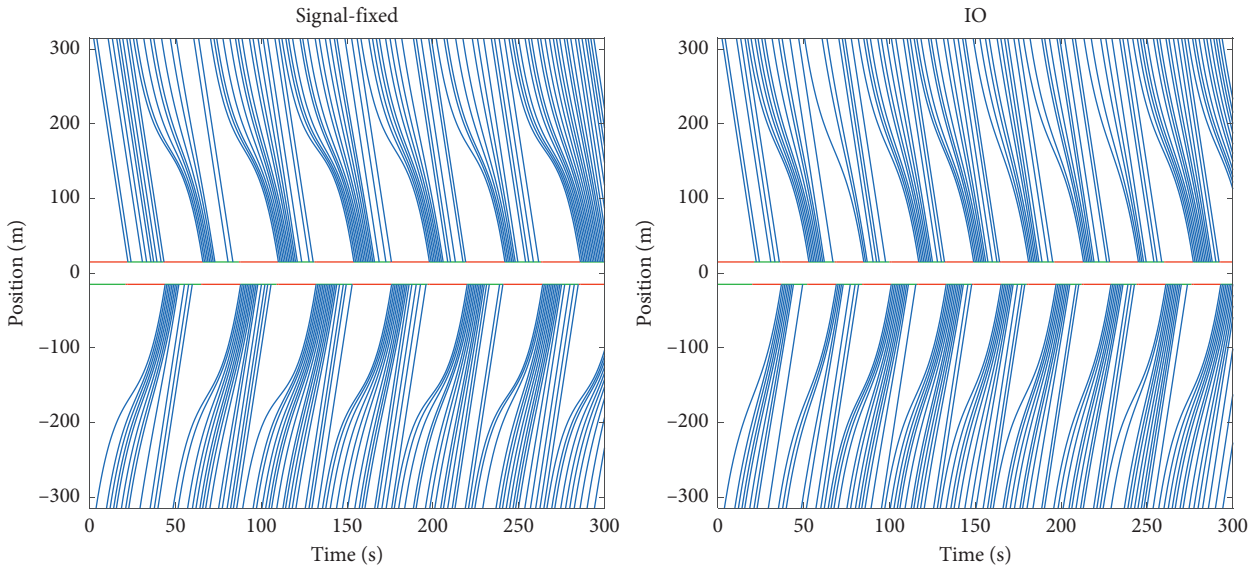

(a)

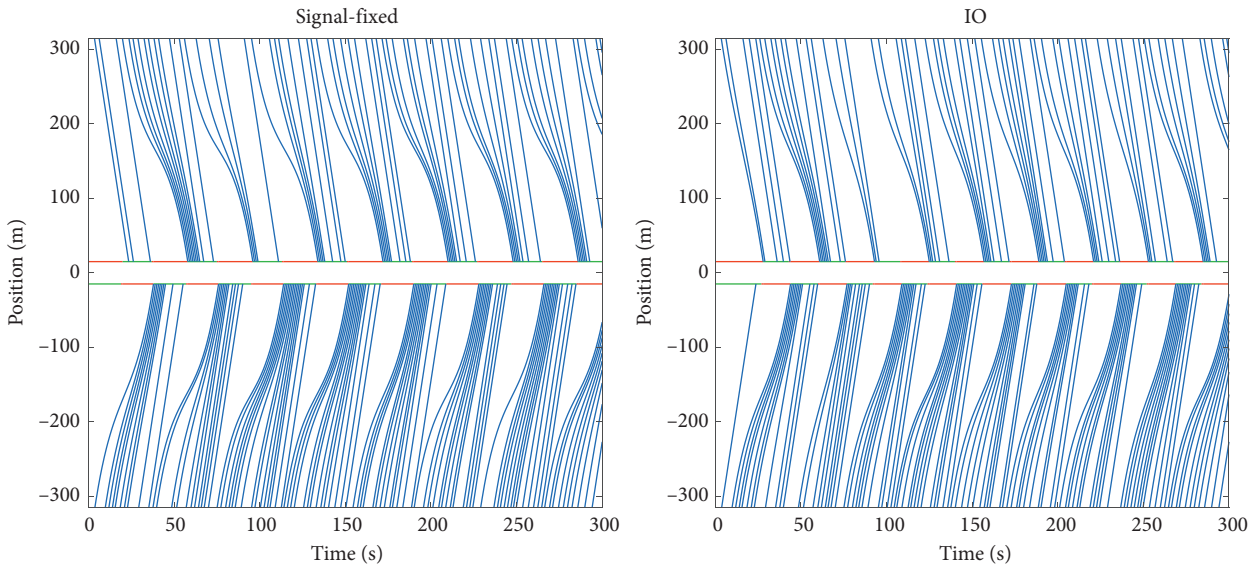

(b)

Figure 3: Continued.

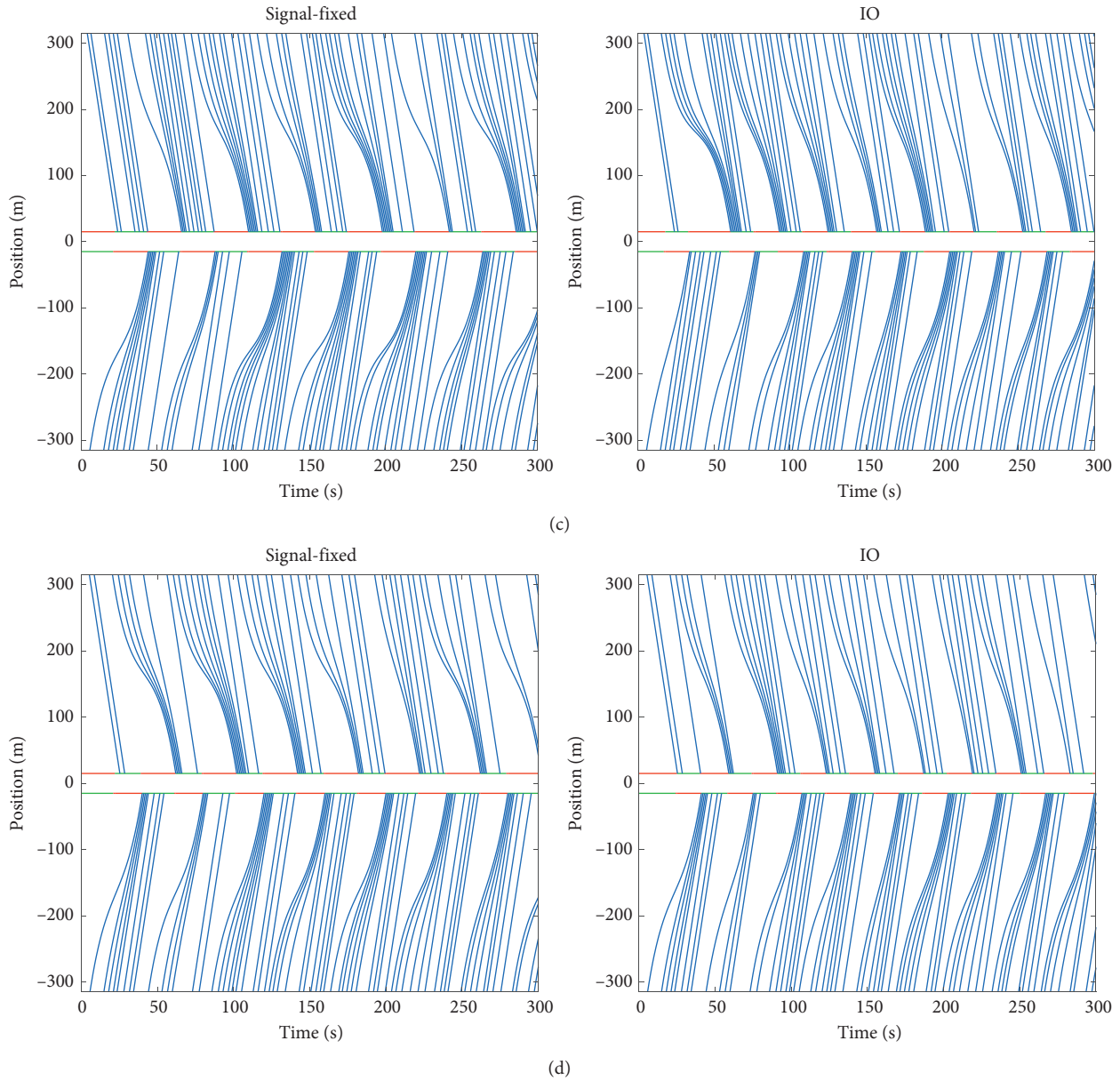

Figure 3: Trajectories of CAVs in arm 1 and 2 as an example. (a) 1200/1200 vph. (b) 1200/800 vph. (c) 800/800 vph. (d) 800/600 vph.

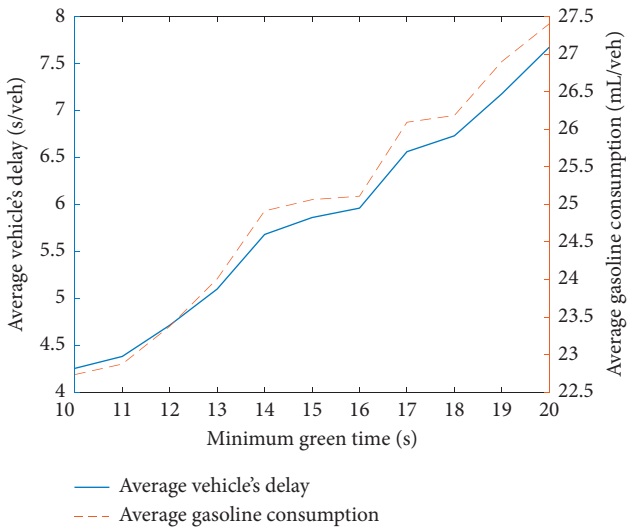

Figure 4: Sensitivity analysis on minimum green time.

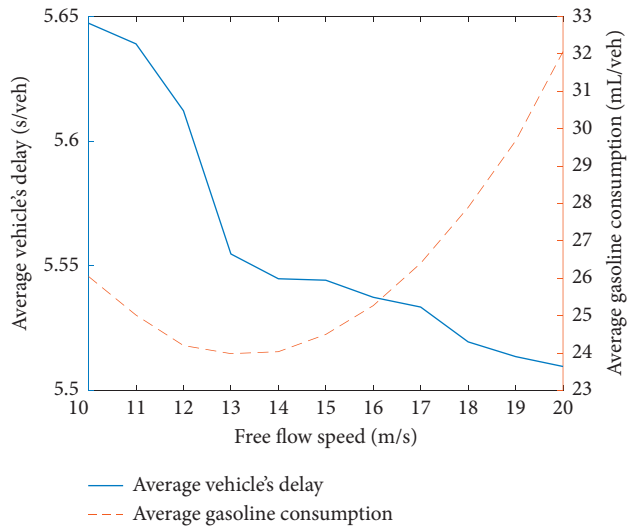

Figure 5: Sensitivity analysis on free-flow speed.

Table 2: The average vehicle's delay and gasoline consumption in different scenarios.

λ_1 (vph)	λ_2 (vph)	Delay (s/veh)			Gasoline consumption (mL/veh)		
		IO	Signal-fixed	Decrease	IO	Signal-fixed	Decrease
1200	1200	5.8598	8.0169	−26.91%	25.0633	27.9663	−10.38%
1200	800	5.4404	6.4440	−15.57%	24.3265	25.6891	−5.30%
800	800	5.0441	6.6516	−24.17%	23.2960	25.4607	−8.50%
800	600	4.9859	6.2673	−20.45%	23.2806	25.0732	−7.15%
Average	5.3326	6.8450	−21.77%	23.9916	26.0473	−7.83%	

behavior [50, 52, 53]. We will improve the proposed model and apply it to multiple intersections or a traffic network in the next step.

Data Availability

The data used to support the findings of this study are included within the article.

Conflicts of Interest

The authors declare that they have no conflicts of interest.

Acknowledgments

This work are supported by the National Natural Science Foundation of China (no. 52002339), the Science and Technology Program of Sichuan Province (2021YJ0535), and the Fundamental Research Funds for the Central Universities (2682021CX058).

References

[1] W. Li and X. Ban, "Connected vehicles based traffic signal timing optimization," *IEEE Transactions on Intelligent Transportation Systems*, vol. 20, no. 12, pp. 4354–4366, 2019.

[2] Z. Yao, B. Zhao, T. Yuan, H. Jiang, and Y. Jiang, "Reducing gasoline consumption in mixed connected automated vehicles environment: a joint optimization framework for traffic signals and vehicle trajectory," *Journal of Cleaner Production*, vol. 265, Article ID 121836, 2020.

[3] B. Schneider, *New Study of Global Traffic Reveals that Traffic is Bad*, City Lab, Los Angeles, CA, USA, 2018.

[4] Z. Li, P. Liu, C. Xu, H. Duan, and W. Wang, "Reinforcement learning-based variable speed limit control strategy to reduce traffic congestion at freeway recurrent bottlenecks," *IEEE Trans. Intell. Transport. Syst.*vol. 18, no. 11, pp. 3204–3217, 2017.

[5] Q. Wan, G. Peng, Z. Li, and F. H. T. Inomata, "Spatiotemporal trajectory characteristic analysis for traffic state transition prediction near expressway merge bottleneck," *Transportation Research Part C: Emerging Technologies*, vol. 117, Article ID 102682, 2020.

[6] A. H. F. Chow, S. Li, and R. Zhong, "Multi-objective optimal control formulations for bus service reliability with traffic signals," *Transportation Research Part B: Methodological*, vol. 103, pp. 248–268, 2017.

[7] F. V Webster, *Traffic Signal Settings*, Department of Scientific and Industrial Research, London, UK, 1958.

[8] Y. Feng, C. Yu, and H. X. Liu, "Spatiotemporal intersection control in a connected and automated vehicle environment," *Transportation Research Part C: Emerging Technologies*, vol. 89, pp. 364–383, 2018.

[9] Y. Feng, K. L. Head, S. Khoshmagham, and M. Zamanipour, "A real-time adaptive signal control in a connected vehicle environment," *Transportation Research Part C: Emerging Technologies*, vol. 55, pp. 460–473, 2015.

[10] Y. Feng, M. Zamanipour, K. L. Head, and S. Khoshmagham, "Connected vehicle-based adaptive signal control and applications," *Transportation Research Record: Journal of the Transportation Research Board*, vol. 2558, no. 1, pp. 11–19, 2016.

[11] B. Beak, K. L. Head, and Y. Feng, "Adaptive coordination based on connected vehicle technology," *Transportation Research Record: Journal of the Transportation Research Board*, vol. 2619, no. 1, pp. 1–12, 2017.

[12] J. Lee, B. Park, I. Yun, and I. Yun, "Cumulative travel-time responsive real-time intersection control algorithm in the connected vehicle environment," *Journal of Transportation Engineering*, vol. 139, no. 10, pp. 1020–1029, 2013.

[13] C. Priemer and B. Friedrich, "A decentralized adaptive traffic signal control using v2i communication data," in *Proceedings of the 2009 12th International IEEE Conference On Intelligent Transportation Systems*, pp. 765–770, St. Louis, MO, USA, October 2009.

[14] Z. Yao, H. Jiang, Y. Cheng, Y. Jiang, and B. Ran, "Integrated schedule and trajectory optimization for connected automated vehicles in a conflict zone," *IEEE Transactions on Intelligent Transportation Systems*, vol. 40, pp. 1–11, 2020.

[15] F. Zhu and S. V. Ukkusuri, "A linear programming formulation for autonomous intersection control within a dynamic traffic assignment and connected vehicle environment," *Transportation Research Part C: Emerging Technologies*, vol. 55, pp. 363–378, 2015.

[16] X. Zeng, X. Sun, Y. Zhang, and L. Quadrifoglio, "Person-based adaptive priority signal control with connected-vehicle information," *Transportation Research Record: Journal of the Transportation Research Board*, vol. 2487, no. 1, pp. 78–87, 2015.

[17] E. Bagheri, B. Mehran, B. Hellinga, and Bruce, "Real-time estimation of saturation flow rates for dynamic traffic signal control using connected-vehicle data," *Transportation Research Record: Journal of the Transportation Research Board*, vol. 2487, no. 1, pp. 69–77, 2015.

[18] K. Tiaprasert, Y. Zhang, X. B. Wang, and X. Zeng, "Queue length estimation using connected vehicle technology for adaptive signal control," *IEEE Transactions on Intelligent Transportation Systems*, vol. 16, no. 4, pp. 2129–2140, 2015.

[19] K. Yang, S. I. Guler, and M. Menendez, "A transit signal priority algorithm under connected vehicle environment," in *Proceedings of the 2015 IEEE 18th International Conference on Intelligent Transportation Systems*, pp. 66–70, Gran Canaria, Spain, October 2015.

[20] Y. Wang, W. Ma, W. Yin, and X. Yang, "Implementation and testing of cooperative bus priority system in connected vehicle

environment," *Transportation Research Record: Journal of the Transportation Research Board*, vol. 2424, no. 1, pp. 48–57, 2014.

[21] H. Jiang, J. Hu, S. An, M. Wang, and B. B. Park, "Eco approaching at an isolated signalized intersection under partially connected and automated vehicles environment," *Transportation Research Part C: Emerging Technologies*, vol. 79, pp. 290–307, 2017.

[22] N. Wan, A. Vahidi, and A. Luckow, "Optimal speed advisory for connected vehicles in arterial roads and the impact on mixed traffic," *Transportation Research Part C: Emerging Technologies*, vol. 69, pp. 548–563, 2016.

[23] Y. Wei, C. Avcı, J. Liu et al., "Dynamic programming-based multi-vehicle longitudinal trajectory optimization with simplified car following models," *Transportation Research Part B: Methodological*, vol. 106, pp. 102–129, 2017.

[24] A. Omidvar, M. Pourmehrab, P. Emami et al., "Deployment and testing of optimized autonomous and connected vehicle trajectories at a closed-course signalized intersection," *Transportation Research Record: Journal of the Transportation Research Board*, vol. 2672, no. 19, pp. 45–54, Article ID 036119811878279, 2018.

[25] W. Zhao, D. Ngoduy, S. Shepherd, R. Liu, and M. Papageorgiou, "A platoon based cooperative eco-driving model for mixed automated and human-driven vehicles at a signalised intersection," *Transportation Research Part C: Emerging Technologies*, vol. 95, pp. 802–821, 2018.

[26] X. He and X. Wu, "Eco-driving advisory strategies for a platoon of mixed gasoline and electric vehicles in a connected vehicle system," *Transportation Research Part D: Transport and Environment*, vol. 63, pp. 907–922, 2018.

[27] A. Ghiasi, X. Li, Z. Huang, and X. Qu, "A joint trajectory and signal optimization model for connected automated vehicles," in *Proceedings of the Transportation Research Board 98th Annual Meeting*, pp. 1–10, Washington, DC, USA, January 2019.

[28] B. Xu, X. J. Ban, Y. Bian et al., "Cooperative method of traffic signal optimization and speed control of connected vehicles at isolated intersections," *IEEE Transactions on Intelligent Transportation Systems*, vol. 20, no. 4, pp. 1390–1403, 2019.

[29] C. Yu, Y. Feng, H. X. Liu, W. Ma, and X. Yang, "Integrated optimization of traffic signals and vehicle trajectories at isolated urban intersections," *Transportation Research Part B: Methodological*, vol. 112, pp. 89–112, 2018.

[30] A. V. Rao, D. A. Benson, C. Darby et al., "Acm transactions on mathematical software Algorithm 902," *GPOPS , A MATLAB Software for Solving Multiple-Phase Optimal Control Problems Using the Gauss Pseudospectral Method*, vol. 37, no. 2, pp. 1–39, 2011.

[31] L. Li and X. Li, "Parsimonious trajectory design of connected automated traffic," *Transportation Research Part B: Methodological*, vol. 119, pp. 1–21, 2019.

[32] X. He, H. X. Liu, and X. Liu, "Optimal vehicle speed trajectory on a signalized arterial with consideration of queue," *Transportation Research Part C: Emerging Technologies*, vol. 61, pp. 106–120, 2015.

[33] X. Wu, X. He, G. Yu, A. Harmandayan, and Y. Wang, "Energy-optimal speed control for electric vehicles on signalized arterials," *IEEE Transactions on Intelligent Transportation Systems*, vol. 16, no. 5, pp. 2786–2796, 2015.

[34] X. T. Yang, K. Huang, Z. Zhang, Z. A. Zhang, and F. Lin, "Eco-driving system for connected automated vehicles: multi-objective trajectory optimization," *IEEE Transactions on Intelligent Transportation Systems*, vol. 1, no. 1–13, 2021.

[35] N. J. Goodall, B. L. Smith, B. Park, and Park, "Traffic signal control with connected vehicles," *Transportation Research Record: Journal of the Transportation Research Board*, vol. 2381, no. 1, pp. 65–72, 2013.

[36] X. Li, A. Ghiasi, Z. Xu, and X. Qu, "A piecewise trajectory optimization model for connected automated vehicles: exact optimization algorithm and queue propagation analysis," *Transportation Research Part B: Methodological*, vol. 118, pp. 429–456, 2018.

[37] R. Niroumand, M. Tajalli, L. Hajibabai, and A. Hajbabaie, "Joint optimization of vehicle-group trajectory and signal timing: introducing the white phase for mixed-autonomy traffic stream," *Transportation Research Part C Emerging Technologies*, vol. 116, Article ID 102659, 2020.

[38] X. Chang, J. Rong, H. Li, Y. Wu, and X. Zhao, "Impact of connected vehicle environment on driving performance: a case of an extra-long tunnel scenario," *IET Intelligent Transport Systems*, vol. 15, no. 3, pp. 423–431, 2021.

[39] G. Li, S. Fang, J. Ma, and J. Cheng, "Modeling merging acceleration and deceleration behavior based on gradient-boosting decision tree," *Journal of Transportation Engineering, Part A: Systems*, vol. 146, no. 7, Article ID 05020005, 2020.

[40] G. Li, Z. Yang, Q. Yu, J. Ma, and S. Fang, "Characterizing heterogeneity among merging positions: comparison study between random parameter and latent class Accelerated hazard model," *Journal of Transportation Engineering, Part A: Systems*, vol. 147, no. 6, 2021.

[41] Z. Yao, L. Shen, R. Liu, Y. Jiang, and X. Yang, "A dynamic predictive traffic signal control framework in a cross-sectional vehicle infrastructure integration environment," *IEEE Transactions on Intelligent Transportation Systems*, vol. 21, no. 4, pp. 1455–1466, 2020.

[42] Z. Yao, Y. Jiang, B. Zhao, X. Luo, and B. Peng, "A dynamic optimization method for adaptive signal control in a connected vehicle environment," *Journal of Intelligent Transportation Systems*, vol. 24, no. 2, pp. 184–200, 2020.

[43] Z. Yao, R. Hu, Y. Jiang, and T. Xu, "Stability and safety evaluation of mixed traffic flow with connected automated vehicles on expressways," *Journal of Safety Research*, vol. 75, pp. 262–274, 2020.

[44] Z. Yao, R. Hu, Y. Wang, Y. Jiang, B. Ran, and Y. Chen, "Stability analysis and the fundamental diagram for mixed connected automated and human-driven vehicles," *Physica A: Statistical Mechanics and Its Applications*, vol. 533, Article ID 121931, 2019.

[45] Z. Yao, T. Xu, Y. Jiang, and R. Hu, "Linear stability analysis of heterogeneous traffic flow considering degradations of connected automated vehicles and reaction time," *Physica A: Statistical Mechanics and Its Applications*, vol. 561, Article ID 125218, 2021.

[46] J. N. Hooker, "Optimal driving for single-vehicle fuel economy," *Transportation Research Part A: General*, vol. 22, no. 3, pp. 183–201, 1988.

[47] R. Akcelik, "Efficiency and drag in the power-based model of fuel consumption," *Transportation Research Part B: Methodological*, vol. 23, no. 5, pp. 376–385, 1989.

[48] K. Ahn, *Microscopic Fuel Consumption and Emission Modeling*, " Virginia Polytechnic Institute and State University, Blacksburg, VA, USA, 1998.

[49] S. Sen and K. L. Head, "Controlled optimization of phases at an intersection," *Transportation Science*, vol. 31, no. 1, pp. 5–17, 1997.

[50] G. Li and J. Cheng, "Exploring the effects of traffic density on merging behavior," *IEEE Access*, vol. 7, pp. 51608–51619, 2019.

[51] D. Husch and A. John, *Synchro 6: Traffic Signal Software, User Guide*, Trafficware, Albany, CA, USA, 2003.
[52] G. Li, J. Ma, and Q. Shen, "Modeling of merging decision during execution period based on random forest," *Journal of Advanced Transportation*, vol. 2021, Article ID 6654096, 11 pages, 2021.
[53] G. Li, Y. Pan, Z. Yang, and J. Ma, "Modeling vehicle merging position selection behaviors based on a finite mixture of linear regression models," *IEEE Access*, vol. 7, pp. 158445–158458, 2019.